European Cells and Materials Vol. 26 2013 (pages 222-233) DOI: 10.22203/eCM.v026a16 ISSN 1473-2262

GENERATION OF CO-CULTURE SPHEROIDS AS VASCULARISATION UNITS FOR BONE TISSUE ENGINEERING

R. Walser[1,3,§], W. Metzger[2,3,§,*], A. Görg[1,2,3], T. Pohlemann[2,3], M.D. Menger[1,3] and M.W. Laschke[1,3]

[1]Institute for Clinical and Experimental Surgery, Saarland University, 66421 Homburg/Saar, Germany
[2]Department of Trauma, Hand, and Reconstructive Surgery, Saarland University, 66421 Homburg/Saar, Germany.
[3]CRC Homburg, Collaborative Research Centre, AO Foundation, Saarland University, 66421 Homburg/Saar, Germany.

[§]These authors contributed equally to this work.

Abstract

Cell spheroids represent attractive building units for bone tissue engineering, because they provide a three-dimensional environment with intensive direct cell-cell contacts. Moreover, they allow for co-culture of both osteoblasts and vessel-forming cells, which may markedly increase their survival and vascularisation after transplantation. To test this hypothesis, we generated co-culture spheroids by aggregating different combinations of primary human osteoblasts (HOB), human dermal microvascular endothelial cells (HDMEC) and normal human dermal fibroblasts (NHDF) using the liquid overlay technique. Mono-culture spheroids consisting either of HOB or HDMEC served as controls. After *in vitro* characterisation, the different spheroids were transplanted into dorsal skinfold chambers of CD1 nu/nu mice to study *in vivo* their viability and vascularisation over a 2-week observation period by means of repetitive intravital fluorescence microscopy and immunohistochemistry. *In vitro*, co-culture spheroids containing HDMEC rapidly formed dense tubular vessel-like networks within 72 h and exhibited a significantly decreased rate of apoptotic cell death when compared to mono-culture HDMEC spheroids. After transplantation, these networks interconnected to the host microvasculature by external inosculation. Of interest, this process was most pronounced in HOB-HDMEC spheroids and could not further be improved by the addition of NHDF. Accordingly, HOB-HDMEC spheroids were larger when compared to the other spheroid types. These findings indicate that HOB-HDMEC spheroids exhibit excellent properties to preserve viability and to promote proliferation and vascularisation. Therefore, they may be used as functional vascularisation units in bone tissue engineering for the seeding of scaffolds or for the vitalisation of non-healing large bone defects.

Keywords: Spheroid; co-culture; bone; tissue engineering; vascularisation; inosculation; apoptosis; dorsal skinfold chamber; intravital fluorescence microscopy.

[*]Address for correspondence:
Wolfgang Metzger
Department of Trauma, Hand and Reconstructive Surgery
Saarland University, Building 57
66421 Homburg, Germany
Telephone Number: + 49 6841 1647875
FAX Number: + 49 6841 1647801
E-mail: johann-wolfgang.metzger@uks.eu

Introduction

Reconstruction of critical sized bone defects represents a daily challenge in traumatology and often requires bone grafting. At present, the transplantation of freshly isolated autologous bone is considered to be the golden standard, although it bears substantial drawbacks like limited graft availability and significant donor-site morbidity (Fröhlich *et al*., 2008). To overcome these problems, bone tissue engineering may be a promising alternative. Despite considerable progress in this field during the last two decades, however, bone tissue engineering approaches have not yet been translated into clinical practice (Amini *et al*., 2012). It is widely recognised that this is primarily due to an insufficient blood supply of both the implanted tissue construct and the defect site (Amini *et al*., 2012). Accordingly, there is an urgent need for the development of improved vascularisation strategies (Laschke and Menger, 2012). To provide optimal conditions for the development of new microvessels in bone tissue constructs, it may be advantageous to mimic the physiological milieu of natural bone. This involves the interaction of endothelial cells with osteoblasts in a co-culture setup (Santos *et al*., 2009). In addition, the cells may be aggregated to three-dimensional spheroids, which enable intensive direct cell-cell contacts and, thus, are superior to conventional monolayer approaches (Ivascu and Kubbies, 2006). In fact, spheroids have been shown to be more resistant against hypoxia and apoptotic cell death (Bhang *et al*., 2011). Moreover, they secrete higher levels of pro-angiogenic growth factors such as vascular endothelial growth factor (VEGF) and fibroblast growth factor (FGF)-2 (Bhang *et al*., 2011). In line with these findings, we could recently demonstrate that polyurethane scaffolds, which are seeded with spheroids consisting of murine adipose-derived mesenchymal stem cells, exhibit a markedly improved vascularisation when compared to cell-seeded control scaffolds (Laschke *et al*., 2013).

Accordingly, the aim of the present study was to generate spheroid-based individual vascularisation units for bone tissue engineering by aggregating different combinations of primary human osteoblasts (HOB), human dermal microvascular endothelial cells (HDMEC) and normal human dermal fibroblasts (NHDF) in form of co-culture spheroids. HOB are immature osteoblasts, which can differentiate into a mature, bone-forming phenotype (Metzger *et al*., 2013). Endothelial cells are able to form tubular vessel-like structures when embedded as spheroids in a three-dimensional collagen gel (Korff

et al., 2001). Finally, NHDF are an important source of proteins of the extracellular matrix (Klingberg *et al*., 2013), and, therefore, contribute to the stabilisation of newly formed microvessels (Nicosia *et al*., 2011).

The vascularisation of the generated spheroids was analysed in the mouse dorsal skinfold chamber model. This model allows for the repetitive *in vivo* evaluation of angiogenesis and vascularisation by means of intravital fluorescence microscopy and immunohistochemistry (Menger *et al*., 2002; Laschke *et al*., 2011). Thereby, blood vessel formation in response to transplanted tissues and implanted biomaterials can easily be detected due to the fact that angiogenesis does normally not occur in empty dorsal skinfold chambers (Rücker *et al*., 2006). Mono-culture spheroids consisting of HOB or HDMEC served as controls.

Materials and Methods

Cell culture

HOB, HDMEC and NHDF are commercially available primary cells (PromoCell, Heidelberg, Germany), which were used in this study up to passage eight. All three cell types were expanded in master cell banks to ensure standardised conditions for subsequent cell culture experiments. HOB were cultivated at 37 °C, 95 % humidity and 5 % CO_2 until near-confluence in Dulbecco's Modified Eagle Medium (DMEM; PAA, Cölbe, Germany) supplemented with 15 % foetal calf serum (FCS, PAA), whereas HDMEC were cultivated in endothelial cell growth medium MV (PromoCell) and NHDF were cultivated in Quantum 333 (PAA) using 75 cm^2 tissue flasks (Greiner Bio One, Frickenhausen, Germany). Standard trypsination procedures were used to detach the cells.

Generation of spheroids

Spheroids were generated using the liquid overlay technique, as previously described in detail (Metzger *et al*., 2011). Mono-culture spheroids containing 100 % HOB or 100 % HDMEC were compared with co-culture spheroids containing HOB-HDMEC (50 % HOB, 50 % HDMEC) or HOB-HDMEC-NHDF (50 % HOB, 25 % HDMEC, 25 % NHDF), respectively. For the generation of spheroids, an 1 % agarose stock solution (Sigma-Aldrich, Taufkirchen, Germany) was prepared in distilled water and was sterilised by autoclaving. Prior to the seeding of cells, the agarose was melted in a microwave oven. The bottom of 96 flat-bottomed well plates (Greiner Bio One) was coated with 50 µL of liquid agarose, which served as a non-adherent surface. After cooling down the plates for 1.5 h 50,000 cells were seeded in a volume of 100 µL cell culture medium. The composition of the medium reflected the cellular composition of the spheroids. The seeded cells could not adhere to the agarose coating and, thus, spontaneously aggregated to three-dimensional spheroids, which were harvested after 72 h.

Dorsal skinfold chamber model

The vascularisation of the different spheroids was analysed in the mouse dorsal skinfold chamber model by means of intravital fluorescence microscopy (Laschke *et al.,* 2011). All animal experiments were approved by the local governmental animal care committee and were conducted in accordance with the German legislation on protection of animals and the NIH Guidelines for the Care and Use of Laboratory Animals (NIH Publication #85-23 Rev. 1985).

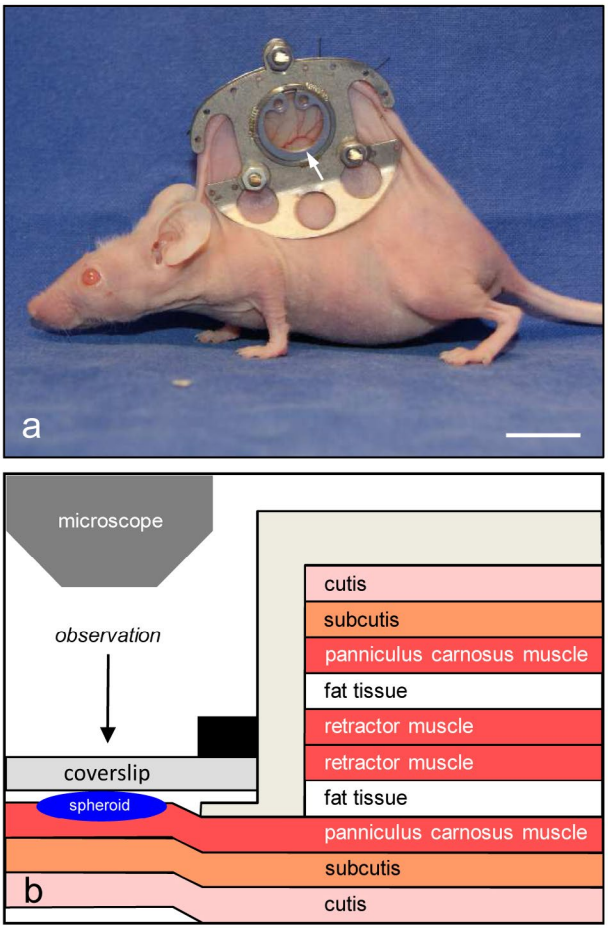

Fig. 1. (**a**) CD1 nu/nu mouse with a dorsal skinfold chamber (chamber weight ~ 2 g). Within the observation window (arrow) all segments of the microcirculation including arterioles, capillaries, and venules of the striated skin muscle and subcutaneous tissue can be analysed using intravital fluorescence microscopy. Scale bar: 1.3 cm. (**b**) Schematic figure displaying the different tissue layers contained within the chamber preparation, including striated skin muscle (panniculus carnosus muscle), subcutis, and cutis. In the present study, the spheroids were transplanted onto the striated skin muscle, which was covered with a removable coverslip incorporated into one of the titanium frames.

Dorsal skinfold chambers were implanted in CD1 nu/nu mice (10-12 weeks old, 25-30 g body weight; Charles River Laboratories GmbH, Sulzfeld, Germany). The mice were kept in single individually ventilated cages at a temperature of 22-24 °C, a relative humidity of 60-65 % and a 12 h day-night cycle. The mice had free access to standard laboratory chow (Altromin, Lage, Germany) and drinking water *ad libitum*.

For the implantation of the dorsal skinfold chamber, the mice were anaesthetised by an intraperitoneal injection of 75 mg/kg ketamine (Ursotamin®; Serumwerk, Bernburg,

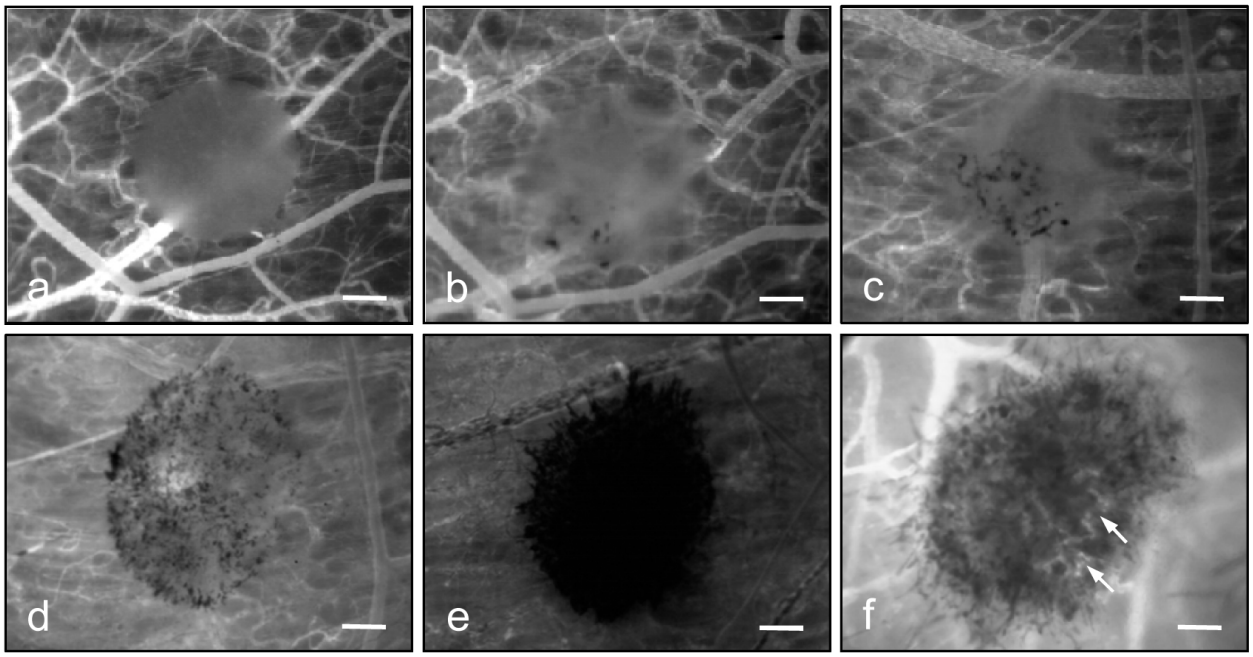

Fig. 2. **(a-e)** Intravital fluorescence microscopic images of transplanted spheroids in the dorsal skinfold chamber of CD1 nu/nu mice, exhibiting different degrees of intrinsic vascularisation according to the following semiquantitative score: 0 = no signs of intrinsic vascularisation (**a**); 1 = intrinsic vascularisation of less than 25 % of the spheroid area (**b**); 2 = intrinsic vascularisation of less than 50 % of the spheroid area (**c**); 3 = intrinsic vascularisation of 50-100 % of the spheroid area (**d**); 4 = intrinsic vascularisation excessing the borders of the spheroid (**e**). (**f**) Example of a spheroid, which exhibits FITC dextran-perfused microvessels (arrows) at day 14 after transplantation. Blue-light epi-illumination with contrast enhancement by 5 % FITC-labelled dextran 150,000 *i.v.*. Scale bars: (a-e) = 220 µm; (**f**) = 140 µm.

Germany) and 25 mg/kg xylazine (Rompun®; Bayer, Leverkusen, Germany). Subsequently, two symmetrical titanium frames were implanted on the extended dorsal skinfold of the animals, so that they sandwiched the double layer of skin (Fig. 1a). One layer of skin was completely removed in a circular area of ~15 mm in diameter, and the remaining tissue (consisting of striated skin muscle, subcutaneous tissue and skin) were covered with a removable coverslip incorporated into one of the titanium frames (Fig. 1b). After the preparation, the mice were allowed to recover from anaesthesia and surgery for 72 h.

Thereafter, spheroids were transplanted into the chambers. For this purpose, the spheroids were stained for 20 min in DMEM (10 % FCS, 100 U/mL penicillin, 0.1 mg/mL streptomycin; PAA) supplemented with the fluorescent vital dye bisbenzimide (2 µg/mL; H33342; Sigma-Aldrich). On ultraviolet epi-illumination, this dye is characterised by a bright blue fluorescence with only little bleaching that persists through several cell generations. Accordingly, the specific fluorescence/background fluorescence ratio was high enough to precisely delineate the stained spheroids from the surrounding non-stained host tissue within the chamber. In addition, this staining allowed for the quantification of apoptotic cells inside the spheroids, which could be identified by an increased chromatin condensation and fragmentation (Vollmar *et al*., 2001). After rinsing in phosphate buffered saline (PBS), three spheroids were carefully placed onto the host striated muscle tissue of each dorsal skinfold chamber with a maximal distance to each other and the chamber was closed again with a new coverslip.

Intravital fluorescence microscopy and image analysis

For *in vivo* microscopic analyses, the anaesthetised mice were placed in right lateral decubital position on a Plexiglas stage. For the visualisation of microvessels by contrast enhancement of the blood plasma, 0.05 mL 5 % fluorescein-isothiocyanate (FITC)-labelled dextran (molecular weight: 150,000 Da; Sigma-Aldrich) was injected intravenously (i.v.) *via* the retrobulbary space. Subsequently, the mice were positioned under a Zeiss Axiotech microscope (Zeiss, Oberkochen, Germany), which was equipped with 5x, 10x, 20x and 50x long-distance objectives (Zeiss) and a 100 W mercury lamp attached to an epi-illumination filter block for blue, green and ultraviolet light. The microscopic images were transferred by a charge-coupled device video camera (FK6990; Pieper, Schwerte, Germany) to a 14 inch video screen (KV-14CT1E; Sony, Tokyo, Japan) and recorded on DVD for off-line evaluation.

The microscopic images were analysed by means of the computer-assisted analysis system CapImage (Zeintl, Heidelberg, Germany). The analyses included the determination of the spheroid area at day 14 (given in % of the initial area at day 0) and the number of apoptotic cells inside the grafts, which were assessed in 3-4 high power fields (HPF) per spheroid directly as well as at day 3 after transplantation into the dorsal skinfold

chamber. In addition, intrinsic vascularisation was defined as the presence of newly formed microvessels inside the spheroids, which did not originate from ingrowing microvessels of the host tissue. These microvessels were filled with erythrocytes over time by developing interconnections to the surrounding host microvasculature. However, they were not perfused with FITC dextran-labelled blood plasma at the time point of microscopic observation and, thus, appeared as black structures in the grafts. The intrinsic vascularisation was evaluated by the following semiquantitative score: 0 = no signs of intrinsic vascularisation; 1 = intrinsic vascularisation of less than 25 % of the spheroid area; 2 = intrinsic vascularisation of less than 50 % of the spheroid area; 3 = intrinsic vascularisation of 50-100 % of the spheroid area; 4 = intrinsic vascularisation excessing the borders of the spheroid (Figs. 2a-e). Finally, we assessed the take rate of the grafts, i.e. the percentage of spheroids, which exhibited FITC dextran-perfused microvessels at day 14 after transplantation into the dorsal skinfold chamber (Fig. 2f).

Experimental protocol

Dorsal skinfold chambers were prepared in a total of 32 CD1 nu/nu mice. The animals were randomly divided into 4 groups (n = 8 per group). After 72 h, three spheroids of identical composition were transplanted into each chamber. These spheroids consisted of 100 % HOB, 100 % HDMEC, HOB-HDMEC (50 % / 50 %) or HOB-HDMEC-NHDF (50 % / 25 % / 25 %). Intravital fluorescence microscopy was performed immediately as well as 3, 6, 10 and 14 days after spheroid transplantation. At the end of the *in vivo* experiments, the animals were sacrificed with an overdose of the anaesthetic and the dorsal skinfold preparations were excised for further immunohistochemical analyses.

Immunohistochemistry

To analyse the distribution and organisation of CD31-positive HDMEC in the different spheroid types, 12 freshly generated spheroids of each group were embedded in 100 µL Hepato-quick (Roche, Basel, Switzerland), 50 µL human citrate plasma (produced by the Institute for Clinical and Experimental Surgery, Homburg/Saar, Germany) and 10 µL calcium chloride (10 %; Merck, Darmstadt, Germany) for 20 min. Subsequently, the spheroids were fixed overnight in 4 % formaldehyde phosphate buffer (Roti® Histofix; Carl Roth, Karlsruhe, Germany). After dehydration, the tissue was embedded in paraffin (Carl Roth) and cut into 5 µm-thick sections. The sections were stained with a monoclonal rabbit-anti-human antibody against CD31 (1:30; Abcam, Cambridge, UK) followed by a goat-anti-rabbit-Cy3 antibody (1:50; Jackson ImmunoResearch Laboratories, West Grove, PA, USA), which served as secondary antibody. On each section, cell nuclei were stained with bisbenzimide (1:500; H33342; Sigma-Aldrich) to merge the images exactly. The sections were examined using a BZ-8000 microscope (Keyence, Osaka, Japan).

To quantify the number of cleaved caspase-3-positive apoptotic cells inside the spheroids, additional sections were stained with a polyclonal rabbit-anti-mouse antibody against cleaved caspase-3 (1:100; Cell Signaling Technology, Danvers, MA, USA) followed by a peroxidase-conjugated goat-anti-rabbit antibody (1:100; Jackson ImmunoResearch Laboratories), which served as secondary antibody. Diaminobenzidine served as chromogen. The sections were counterstained with Hemalaun. The sections were examined using light microscopy (BX60; Olympus, Hamburg, Germany). In each spheroid, the number of apoptotic cells were assessed in 2-3 HPF and are given in % of the total cell number/HPF. Because some spheroids were lost during the histological processing, the number of analysed spheroids ranged between 5-8 in the individual groups.

In addition, spheroid-containing dorsal skinfold chamber preparations were carefully excised at the end of the *in vivo* experiments, i.e. at day 14 after spheroid transplantation, and embedded in paraffin after formalin fixation. To study the origin of newly formed microvessels inside the spheroids (intrinsic human vascularisation *vs*. in-growing microvessels from the surrounding murine tissue), 5 µm-thick sections were stained with a monoclonal rabbit-anti-human antibody (1:200; Abcam) and a monoclonal rat-anti-mouse antibody (1:30; Dianova, Hamburg, Germany) against CD31 followed by a goat-anti-rabbit-Cy3 antibody (1:400; Jackson ImmunoResearch Laboratories) and a goat-anti-rat-Alexa 488 antibody (1:400; Invitrogen, Carlsbad, CA, USA), which served as secondary antibodies. On each section, cell nuclei were stained with bisbenzimide (1:500; H33342; Sigma-Aldrich). The sections were examined using the BZ-8000 microscope (Keyence) for the quantitative analysis of the density of human and murine microvessels inside the spheroids given in mm^{-2}.

Statistics

After testing the data for normal distribution and equality of variances, differences between the groups were analysed by one way ANOVA followed by the Student-Newman-Keuls-test (SigmaStat; Jandel Corporation, San Rafael, CA, USA). In case of not-normally distributed data, differences between groups were analysed by Kruskal-Wallis one way ANOVA on Ranks followed by the Dunn's test according to the Bonferroni principle. Statistical significance was accepted for a value of $p < 0.05$. All data are given as means ± SEM.

Results

Cellular organisation and apoptotic cell death in freshly generated spheroids

Using the liquid overlay technique, it was possible to generate three-dimensional mono-culture spheroids of HOB and HDMEC as well as co-culture spheroids of HOB-HDMEC and HOB-HDMEC-NHDF under highly standardised conditions. After 72 h, the spheroids were stable and exhibited a homogeneous round shape. As expected, HOB spheroids did not contain any CD31-positive cells (Figs. 3a-c), whereas all cells in HDMEC spheroids strongly expressed the endothelial marker CD31

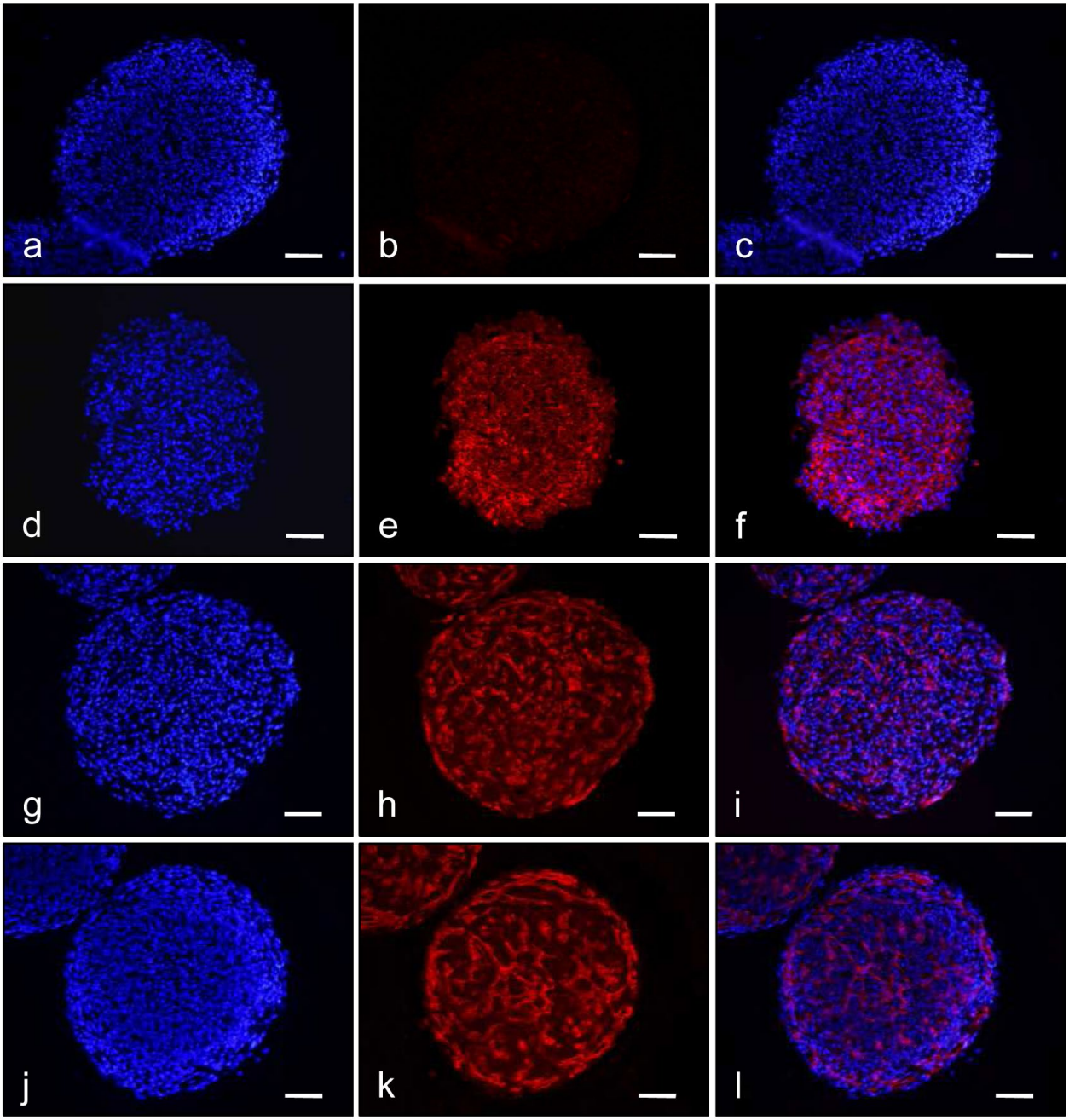

Fig. 3. Immunfluorescence microscopy images of HOB spheroids (**a-c**), HDMEC spheroids (**d-f**), HOB-HDMEC spheroids (**g-i**) and HOB-HDMEC-NHDF spheroids (**j-l**) after generation by the liquid overlay technique. Sections are stained with bisbenzimide to identify cell nuclei (**a**, **d**, **g**, **j**, blue) and an antibody against human CD31 (**b**, **e**, **h**, **k**, red). **c**, **f**, **i** and **l** display merges of (**a**, **b**), (**d**, **e**), (**g**, **h**) and (**j**, **k**). Scale bars: 120 µm.

(Figs. 3d-f). Both types of co-culture spheroids contained CD31-positive HDMEC. However, in contrast to the mono-culture spheroids (Fig. 3d-f), the HDMEC were organised in form of a dense network of tubular vessel-like structures in the co-culture spheroids (Figs. 3g-l).

Immunohistochemical detection of cleaved caspase-3 revealed that HDMEC spheroids exhibited a significantly increased number of apoptotic cells when compared to the other spheroid types (Fig. 4). This clearly indicates that HDMEC are much more susceptible to apoptotic cell death than HOB mono-cultures. Moreover, co-culturing of HDMEC with HOB or HOB-NHDF is an efficient strategy to prevent HDMEC apoptotic cell death.

Area and apoptotic cell death of transplanted spheroids

After transplantation into the dorsal skinfold chamber, the bisbenzimide-stained spheroids of all four groups could easily be delineated from the surrounding non-stained host tissue within the chamber due to their bright fluorescence signal in ultraviolet epi-illumination (Figs. 5a-d). In addition, the bisbenzimide staining allowed for the quantification of apoptotic cells inside the spheroids, which could be identified by an increased chromatin condensation and fragmentation (Figs. 5e-h). In line with our immunohistochemical results, this analysis revealed an increased number of apoptotic cells in HDMEC

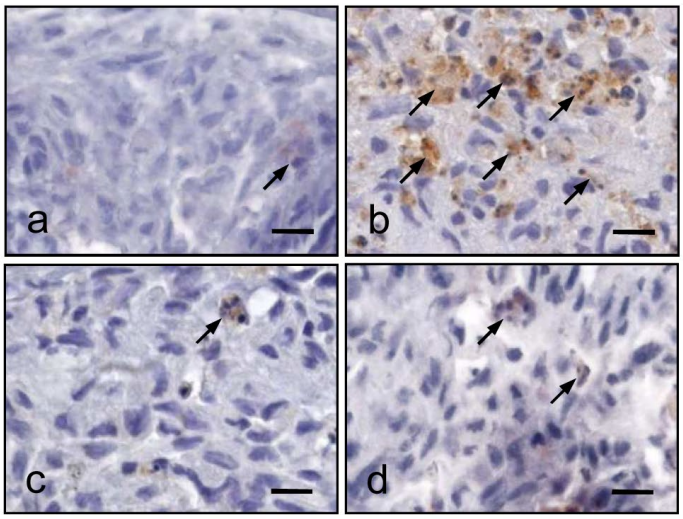

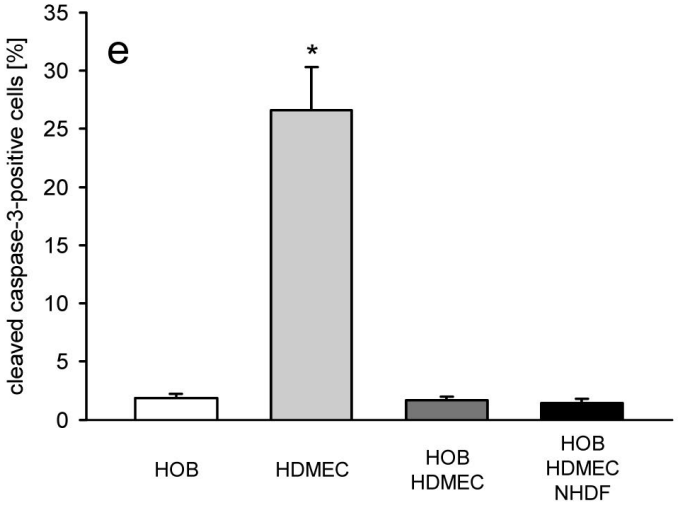

Fig. 4. (**a-d**) Cleaved caspase-3-stained sections of a HOB spheroid (**a**), a HDMEC spheroid (**b**), a HOB-HDMEC spheroid (**c**) and a HOB-HDMEC-NHDF spheroid (**d**) after generation by the liquid overlay technique. Note that the HDMEC spheroid contains a markedly increased number of apoptotic cells (**b**, arrows) when compared to the other spheroid types (**a**, **c**, **d**, arrows). Scale bars: 12 µm. (**e**) Cleaved caspase-3-positive cells (%) inside HOB spheroids (white bar, n = 8), HDMEC spheroids (light grey bar, n = 7), HOB-HDMEC spheroids (dark grey bar, n = 7) and HOB-HDMEC-NHDF spheroids (black bar, n = 5). Mean ± SEM; *$p < 0.05$ *vs*. HOB, HOB-HDMEC and HOB-HDMEC-NHDF.

spheroids directly as well as 3 days after transplantation when compared to the other spheroid types (Figs. 5e-i). Of interest, the area of HOB-HDMEC spheroids at day 14 was significantly increased when compared to day 0, whereas the spheroids of the other groups did not show marked changes in area (Fig. 5j).

Vascularisation of transplanted spheroids

Repetitive intravital fluorescence microscopy revealed the presence of tubular vessel-like structures within all spheroid types, which contained HDMEC. Of interest, these structures were not perfused with FITC dextran-labelled blood plasma at the time point of microscopic observation and therefore appeared black in blue-light epi-illumination (Figs. 2b-e). However, they contained erythrocytes, giving the spheroids an increasing red appearance during stereo-microscopy of the chambers over time (Fig. 6). We termed this phenomenon as intrinsic vascularisation. As expected, no intrinsic vascularisation could be observed in the group of HOB spheroids due to the absence of endothelial cells inside the grafts (Fig. 7). In contrast, all HDMEC-containing spheroid types exhibited an increase in the semiquantitative score for the assessment of intrinsic vascularisation throughout the observation period of 14 days (Fig. 7). Interestingly, this increase was most pronounced in the HOB-HDMEC spheroids (Fig. 7). Accordingly, individual HOB-HDMEC spheroids even presented with an intrinsic vascularisation between day 6 and day 14 after transplantation that exceeded the spheroid borders and grew out into the surrounding host tissue (Figs. 2e, 6c and 8f). This indicates a strong angiogenic activity of the microvascular networks originating from the grafts' HDMEC. In line with these results, we found that HOB-HDMEC spheroids exhibited a higher take rate of 48.0 ± 13.9 % when compared to HOB-HDMEC-NHDF (20.8 ± 12.5 %) and HDMEC spheroids (10.0 ± 7.9 %). In contrast to the other groups, HOB spheroids did not show any FITC dextran-perfused microvessels at day 14.

At the end of the *in vivo* experiments, the dorsal skinfold chamber preparations were further analysed by immunohistochemistry. For this purpose, sections with spheroids were stained by means of an anti-human and an anti-mouse antibody against the endothelial cell marker CD31 to analyse the vessel origin inside the grafts. According to our intravital microscopic analyses, we found that the HOB spheroids only exhibited a very low density of microvessels of 32 ± 24 mm^{-2}, which were all of murine origin (Figs. 8a and b). As expected, HDMEC

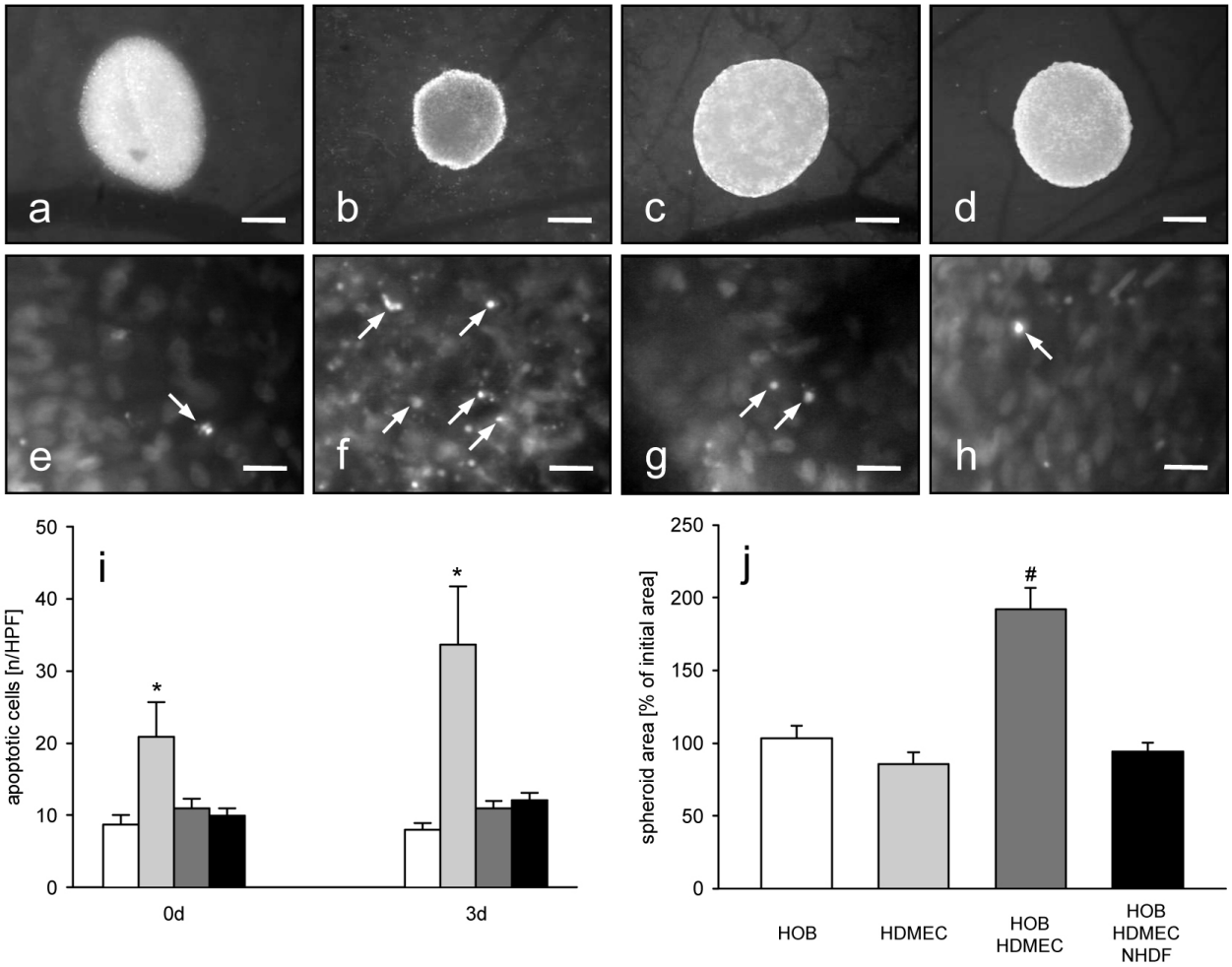

Fig. 5. **(a-h)** Intravital fluorescence microscopic images of a HOB spheroid (**a**, **e**), a HDMEC spheroid (**b**, **f**), a HOB-HDMEC spheroid (**c**, **g**) and a HOB-HDMEC-NHDF spheroid (**d**, **h**) directly (**a-d**) as well as at day 3 (**e-h**) after transplantation into the dorsal skinfold chamber of CD1 nu/nu mice. Note that the bisbenzimide-stained spheroids of all four groups can easily be delineated from the non-stained surrounding host tissue due to their bright fluorescence signal in ultraviolet epi-illumination (**a-d**). At higher magnification, the bisbenzimide staining also allows for the quantification of apoptotic cells inside the spheroids, which can be identified by an increased chromatin condensation and fragmentation (**e-h**, arrows). Scale bars: (**a-d**) = 140 µm; (**e-h**) = 16 µm. **i**, **j**: Apoptotic cells (n/HPF) in spheroids directly (0d) as well as at day 3 after transplantation (**i**) and spheroid area at day 14 (given in % of initial area) (**j**), as assessed by intravital fluorescence microscopy and image analysis. HOB spheroids (white bar, $n = 24$ in 8 animals for quantification of apoptotic cells and spheroid area), HDMEC spheroids (light grey bar, $n = 18$ in 6 animals for quantification of apoptotic cells, $n = 24$ in 8 animals for quantification of spheroid area), HOB-HDMEC spheroids (dark grey bar, $n = 24$ in 8 animals for quantification of apoptotic cells and spheroid area), HOB-HDMEC-NHDF spheroids (black bar, $n = 24$ in 8 animals for quantification of apoptotic cells and spheroid area). *$p < 0.05$ *vs*. HOB; $^{\#}p < 0.05$ *vs*. HOB, HDMEC and HOB-HDMEC-NHDF.

spheroids contained mainly human microvessels with a density of 93 ± 57 mm^{-2} and only in rare cases also murine ones (8 ± 6 mm^{-2}) (Figs. 8c and d). The two types of co-culture spheroids also exhibited a comparable low amount of murine microvessels (HOB-HDMEC: 3 ± 3 mm^{-2} and HOB-HDMEC-NHDF: 6 ± 2 mm^{-2}). However, the microvascular networks inside these spheroids presented with a markedly higher density of human microvessels of 564 ± 165 mm^{-2} (HOB-HDMEC) and 452 ± 83 mm^{-2} (HOB-HDMEC-NHDF) compared to HDMEC spheroids (Figs. 8e-h). Of interest, the lumina of human microvessels inside the three groups of HDMEC-containing spheroids were filled with erythrocytes, indicating that they had developed interconnections to the host microvasculature and were perfused (Figs. 8c-h). In addition, some of the microvessels of human origin could even be detected outside the spheroids penetrating the host striated muscle tissue of the chamber preparation as a sign for their high proliferating activity (Fig. 8f).

Discussion

Cell spheroids represent attractive units for the engineering of tissue constructs, because they provide a physiological three-dimensional environment with intensive cell-cell

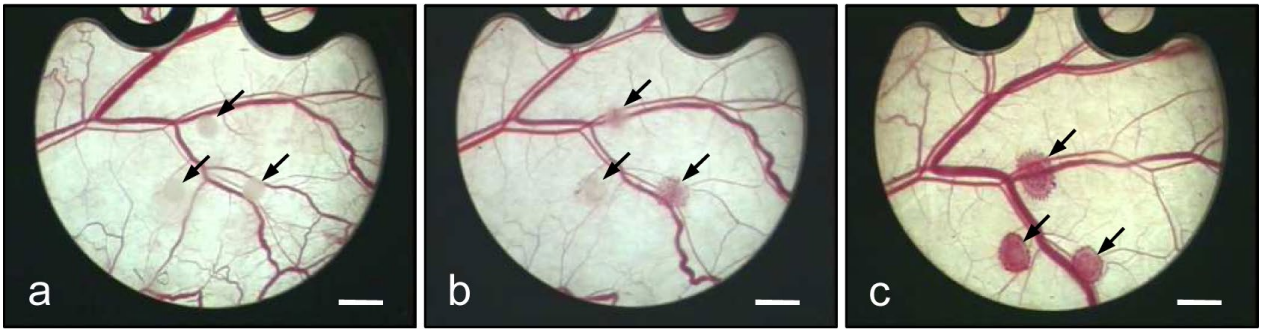

Fig. 6. Stereo-microscopic images of HOB-HDMEC spheroids (arrows) directly (**a**) as well as at day 3 (**b**) and day 14 (**c**) after transplantation into the dorsal skinfold chamber of a CD1 nu/nu mouse. Note that the spheroids exhibit an increasing red appearance over time, indicating that the newly formed microvascular networks of the grafts are progressively filled with erythrocytes. Scale bars: 13 mm.

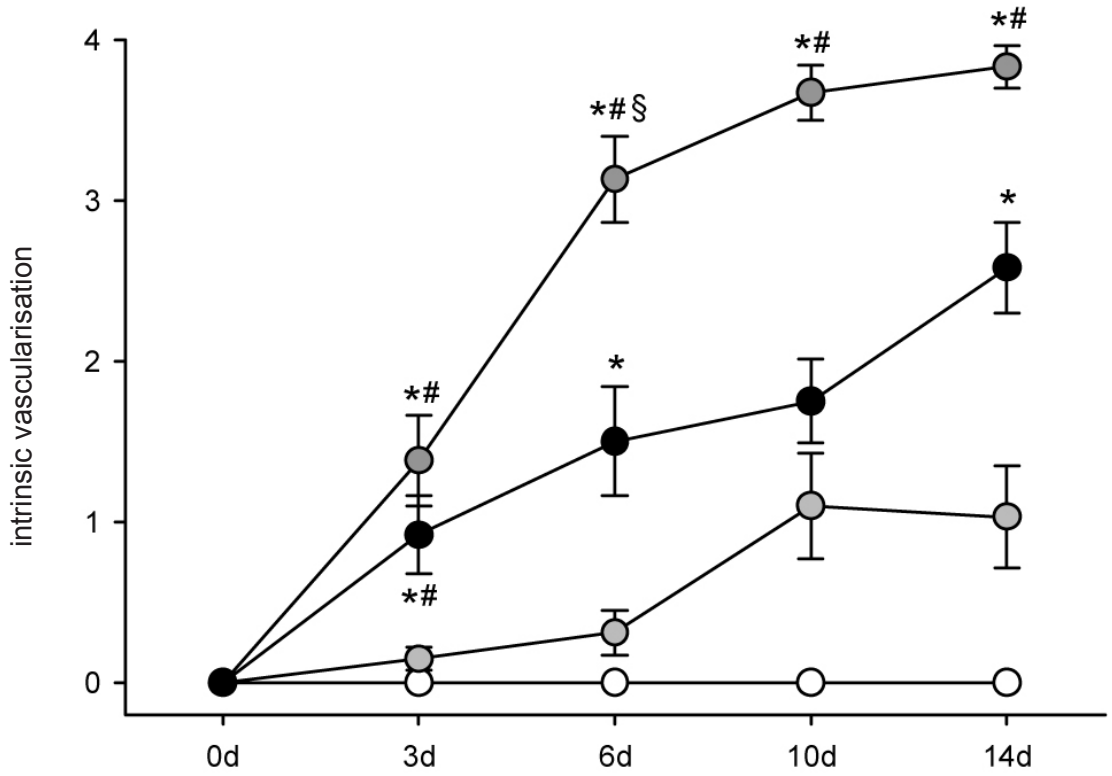

Fig. 7. Intrinsic vascularisation (semiquantitative score as explained in Fig. 2) of HOB spheroids (white circles, $n = 24$ in 8 animals), HDMEC spheroids (light grey circles, $n = 24$ in 8 animals), HOB-HDMEC spheroids (dark grey circles, $n = 24$ in 8 animals) and HOB-HDMEC-NHDF spheroids (black circles, $n = 24$ in 8 animals) directly (0d) as well as at day 3, 6, 10 and 14 after transplantation into the dorsal skinfold chamber of CD1 nu/nu mice, as assessed by intravital fluorescence microscopy. *$p < 0.05$ *vs*. HOB; $^{\#}p < 0.05$ *vs*. HDMEC; $^{\S}p < 0.05$ *vs*. HOB-HDMEC-NHDF.

contacts (Achilli *et al*., 2012). Moreover, they can be generated as co-culture spheroids to simulate tissue-specific interactions of individual cell types with different functions (Wenger *et al*., 2004). In line with these findings, we herein could demonstrate that co-culture spheroids consisting of 50 % HOB and 50 % HDMEC exhibit a high viability, proliferation and vascularisation under *in vivo* conditions.

For the generation of our spheroids, we used the liquid overlay technique. According to previous studies (Metzger *et al*., 2011) this approach allowed for the rapid formation of stable spheroids consisting of defined cell numbers and composition with an excellent reproducibility and rate of yield. Immunohistochemical analyses revealed that spheroids solely consisting of HDMEC exhibited a markedly increased number of apoptotic cells when compared to HOB spheroids, indicating that the endothelial cells in mono-culture were much more susceptible to apoptosis than HOB. However, this could be completely prevented by co-culturing the HDMEC with HOB or HOB-NHDF. This supports the concept that different cell types can activate endothelial cell survival signalling pathways (Brown *et al*., 2004; Wenger *et al*., 2005; Fröhlich *et al*., 2008). *Vice versa*, Steiner *et al*. (2012) recently reported that direct contact to endothelial cells increases the proliferation and reduces low-serum induced apoptosis

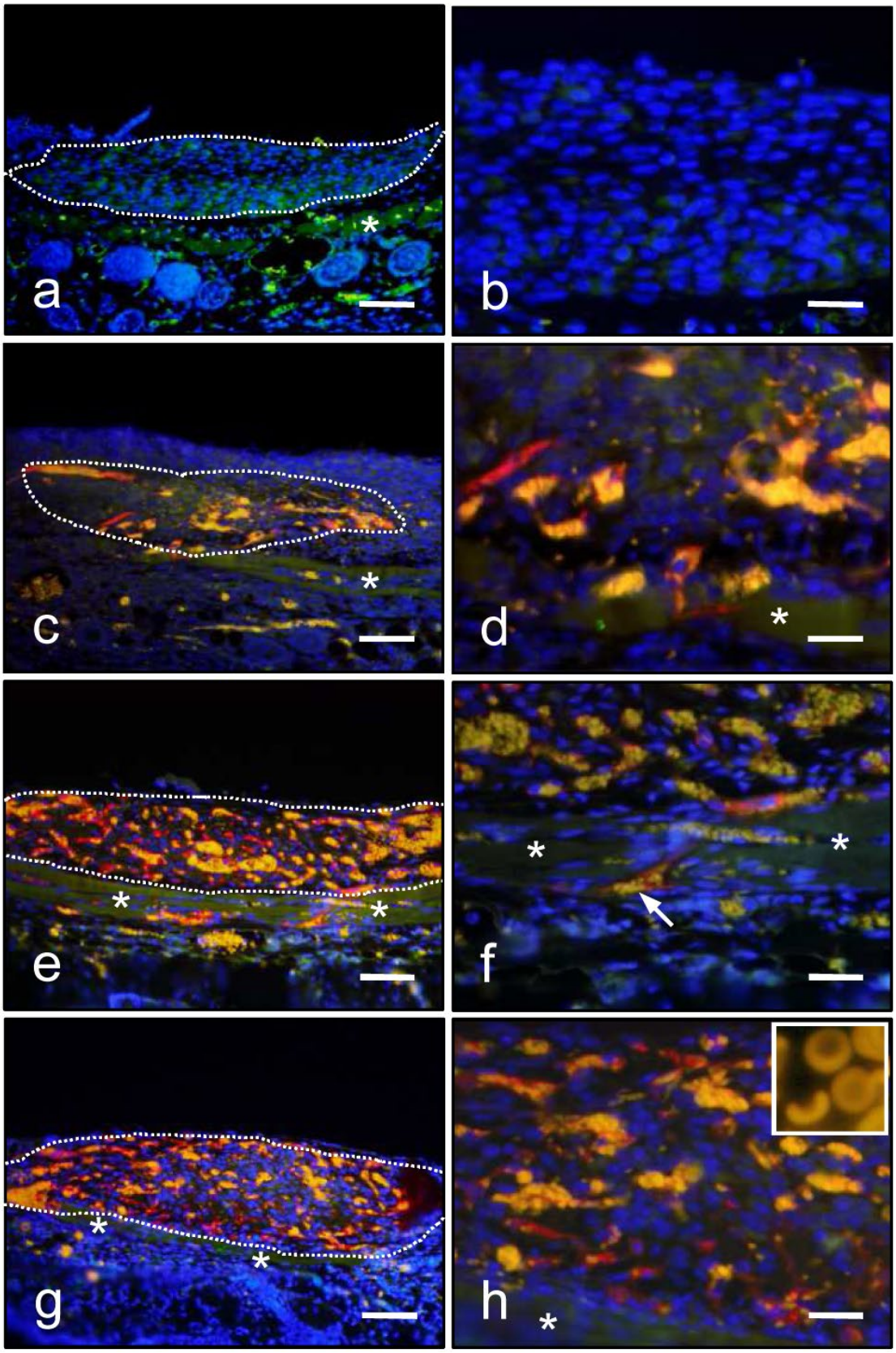

Fig. 8. Immunfluorescence microscopic images of a HOB spheroid (**a**, **b**), a HDMEC spheroid (**c**, **d**), a HOB-HDMEC spheroid (**e**, **f**) and a HOB-HDMEC-NHDF spheroid (**g**, **h**) at day 14 after transplantation onto the host striated muscle tissue (asterisks) of the dorsal skinfold chamber of CD1 nu/nu mice. The borders of the spheroids are marked by dotted line (**a**, **c**, **e**, **g**). Sections were stained with bisbenzimide to identify cell nuclei (blue), an antibody against human CD31 (red) and an antibody against murine CD31 (green). Note that all the spheroids containing HDMEC (**c**-**h**) exhibit functional microvessels of human origin, as indicated by their red colour and presence of unspecifically stained erythrocytes (yellow colour, see insert in **h**) in their lumina. The arrow in f marks a human microvessel penetrating the host striated muscle tissue of the chamber preparation. Scale bars: **a**, **c**, **e**, **g**: 130 µm; **b**, **d**, **f**, **h**: 40 µm.

of cultured HOB. Moreover, co-cultured endothelial cells promote the formation of bone matrix by osteoblasts (Fröhlich *et al*., 2008; Dariima *et al*., 2013). Thus, the co-culture of both cell types may represent a win-win situation, improving cell survival, proliferation and function.

Another major advantage of HDMEC-containing co-culture spheroids is the observation that these spheroids develop dense networks of tubular vessel-like structures under *in vitro* conditions. During the last few years, the generation of intrinsic microvascular networks in tissue constructs has emerged as a favourite vascularisation strategy in tissue engineering (Laschke *et al*., 2006; Lokmic and Mitchell, 2008). In contrast to the time-consuming ingrowth of newly formed blood vessels into tissue constructs at the implantation site, this strategy bears the major advantage that the intrinsic networks are rapidly perfused by inosculation, i.e., the development of interconnections to the host microvasculature (Laschke and Menger, 2012). This may occur inside the implants (internal inosculation) or - in case of a high proliferating and angiogenic activity of the intrinsic networks – also outside the implants (external inosculation) (Laschke *et al*., 2009; Kuehl *et al*., 2013). Herein, we found by immunohistochemical detection of human and murine CD31-positive microvessels that our co-culture spheroids almost exclusively vascularised by external inosculation. They only contained a few ingrowing murine microvessels at day 14, but dense networks of microvessels originating from the HDMEC. Some of these human microvessels could be detected outside the spheroids in the surrounding host tissue. Accordingly, we conclude that the human-derived microvascular networks exhibit a high survival rate, stability and angiogenic activity.

The formation of new blood vessels is a complex process, which does not only involve the activation and sprouting of endothelial cells, but which is also crucially dependent on other cell types, such as pericytes, smooth muscle cells and fibroblasts (Hetheridge *et al*., 2011; Nicosia *et al*., 2011; Ribatti *et al*., 2011). Accordingly, we speculated in the present study that the additional incorporation of NHDF in HOB-HDMEC spheroids may further improve the vascularisation process of the grafts. However, this was not the case. In fact, HOB-HDMEC-NHDF spheroids even presented with a reduced intrinsic vascularisation when compared to the HOB-HDMEC spheroids. Moreover, they exhibited a decreased take rate and a lower microvessel density at day 14. These findings may be explained by the results of an *in vitro* study of Wenger *et al*. (2005) reporting that the sprouting activity of endothelial cells in spheroids is reduced when co-cultured with fibroblasts. This inhibitory effect seems not to be mediated by a paracrine mechanism, but is most likely due to the formation of heterogenic cell contacts between both cell types inside the spheroids (Wenger *et al*., 2005). Therefore, we suggest that the high level of 50 % HDMEC in our HOB-HDMEC spheroids is more advantageous for their vascularisation than the addition of 25 % NHDF. Under physiological conditions, the amount of oxygen, which is required for cell survival, is limited to a diffusion distance of only ~150-200 µm from a supplying blood vessel (Folkman and Hochberg, 1973; Colton, 1995). Thus, the initiation of vascularisation was a major prerequisite for the survival and proliferation of the cells inside the spheroids, which exhibited a thickness larger than 200 µm. In line with this view, HOB-HDMEC spheroids also exhibited a final area at day 14 after transplantation which was significantly increased when compared to the other spheroid types.

In summary, we could demonstrate in the present study that HOB-HDMEC spheroids exhibit a high viability and rapidly develop a functional vascularisation after transplantation. Accordingly, they may be suitable in bone tissue engineering for the seeding of appropriate scaffolds or for the vitalisation of non-healing large bone defects.

Conclusions

In the present study we used primary human cells (HOB, HDMEC and NHDF) to generate mono- and co-culture spheroids. We found that co-cultivation of HDMEC with HOB markedly improves the formation of tubular vessel-like structures within the spheroids and reduces apoptosis of endothelial cells when compared to mono-cultures. After transplantation, HOB-HDMEC spheroids exhibit a high viability and rapidly develop a functional vascularisation by developing interconnections between their intrinsic microvascular networks with the surrounding host microvasculature. Therefore, they represent highly promising vascularisation units for the development of novel bone tissue engineering strategies.

Acknowledgements

We are grateful for the excellent technical assistance of Sandra Schuler, Daniela Sossong and Dominik Walser. This work was financially supported by a grant of the AO Foundation, Switzerland (Collaborative Research Centre, Homburg).

References

Achilli TM, Meyer J, Morgan JR (2012) Advances in the formation, use and understanding of multi-cellular spheroids. Expert Opin Biol Ther **12**: 1347-1360.

Amini AR, Laurencin CT, Nukavarapu SP (2012) Bone tissue engineering: recent advances and challenges. Crit Rev Biomed Eng **40**: 363-408.

Bhang SH, Cho SW, La WG, Lee TJ, Yang HS, Sun AY, Baek SH, Rhie JW, Kim BS (2011) Angiogenesis in ischemic tissue produced by spheroid grafting of human adipose-derived stromal cells. Biomaterials **32**: 2734-2747.

Brown CK, Khodarev NN, Yu J, Moo-Young T, Labay E, Darga TE, Posner MC, Weichselbaum RR, Mauceri HJ (2004) Glioblastoma cells block radiation-induced programmed cell death of endothelial cells. FEBS Lett **565:** 167-170.

Colton CK (1995) Implantable biohybrid artificial organs. Cell Transplant **4**: 415-436.

Dariima T, Jin GZ, Lee EJ, Wall IB, Kim HW (2013) Cooperation between osteoblastic cells and endothelial

cells enhances their phenotypic responses and improves osteoblast function. Biotechnol Lett **35**: 1135-1143.

Folkman J, Hochberg M (1973) Self-regulation of growth in three dimensions. J Exp Med **138**: 745-753.

Fröhlich M, Grayson WL, Wan LQ, Marolt D, Drobnic M, Vunjak-Novakovic G (2008) Tissue engineered bone grafts: biological requirements, tissue culture and clinical relevance. Curr Stem Cell Res Ther **3**: 254-264.

Hetheridge C, Mavria G, Mellor H (2011) Uses of the *in vitro* endothelial-fibroblast organotypic co-culture assay in angiogenesis research. Biochem Soc Trans **39**: 1597-1600.

Ivascu A, Kubbies M (2006) Rapid generation of single-tumor spheroids for high-throughput cell function and toxicity analysis. J Biomol Screen **11**: 922-932.

Klingberg F, Hinz B, White ES (2013) The myofibroblast matrix: implications for tissue repair and fibrosis. J Pathol **229**: 298-309.

Korff T, Kimmina S, Martiny-Baron G, Augustin HG (2001) Blood vessel maturation in a 3-dimensional spheroidal coculture model: direct contact with smooth muscle cells regulates endothelial cell quiescence and abrogates VEGF responsiveness. FASEB J **15**: 447-457.

Kuehl AR, Abshagen K, Eipel C, Laschke MW, Menger MD, Laue M, Vollmar B (2013) External inosculation as a feature of revascularization occurs after free transplantation of murine liver grafts. Am J Transplant **13**: 286-298.

Laschke MW, Harder Y, Amon M, Martin I, Farhadi J, Ring A, Torio-Padron N, Schramm R, Rücker M, Junker D, Häufel JM, Carvalho C, Heberer M, Germann G, Vollmar B, Menger MD (2006) Angiogenesis in tissue engineering: breathing life into constructed tissue substitutes. Tissue Eng **12**: 2093-2104.

Laschke MW, Vollmar B, Menger MD (2009) Inosculation: connecting the life-sustaining pipelines. Tissue Eng Part B Rev **15:** 455-465.

Laschke MW, Vollmar B, Menger MD (2011) The dorsal skinfold chamber: window into the dynamic interaction of biomaterials with their surrounding host tissue. Eur Cell Mater **22**: 147-164.

Laschke MW, Menger MD (2012) Vascularization in tissue engineering: angiogenesis *versus* inosculation. Eur Surg Res **48**: 85-92.

Laschke MW, Schank TE, Scheuer C, Kleer S, Schuler S, Metzger W, Eglin D, Alini M, Menger MD (2013) Three-dimensional spheroids of adipose-derived mesenchymal stem cells are potent initiators of blood vessel formation in porous polyurethane scaffolds. Acta Biomater **9**: 6876-6884.

Lokmic Z, Mitchell GM (2008) Engineering the microcirculation. Tissue Eng Part B Rev **14**: 87-103.

Menger MD, Laschke MW, Vollmar B (2002) Viewing the microcirculation through the window: some twenty years experience with the hamster dorsal skinfold chamber. Eur Surg Res **34**: 83-91.

Metzger W, Sossong D, Bächle A, Pütz N, Wennemuth G, Pohlemann T, Oberringer M (2011) The liquid overlay technique is the key to formation of co-culture spheroids consisting of primary osteoblasts, fibroblasts and endothelial cells. Cytotherapy **13**: 1000-1012.

Metzger W, Schimmelpfennig L, Schwab B, Sossong D, Dorst N, Bubel M, Görg A, Pütz N, Wennemuth G, Pohlemann T, Oberringer M (2013) Expansion and differentiation of human primary osteoblasts in two- and three-dimensional culture. Biotech Histochem **88**: 86-102.

Nicosia RF, Zorzi P, Ligresti G, Morishita A, Aplin AC (2011) Paracrine regulation of angiogenesis by different cell types in the aorta ring model. Int J Dev Biol **55**: 447-453.

Ribatti D, Nico B, Crivellato E (2011) The role of pericytes in angiogenesis. Int J Dev Biol **55**: 261-268.

Rücker M, Laschke MW, Junker D, Carvalho C, Schramm A, Mülhaupt R, Gellrich NC, Menger MD (2006) Angiogenic and inflammatory response to biodegradable scaffolds in dorsal skinfold chambers of mice. Biomaterials 27: 5027-5038.

Santos MI, Unger RE, Sousa RA, Reis RL, Kirkpatrick CJ (2009) Crosstalk between osteoblasts and endothelial cells co-cultured on a polycaprolactone-starch scaffold and the *in vitro* development of vascularization. Biomaterials **30**: 4407-4415.

Steiner D, Lampert F, Stark GB, Finkenzeller G (2012) Effects of endothelial cells on proliferation and survival of human mesenchymal stem cells and primary osteoblasts. J Orthop Res **30**: 1682-1689.

Vollmar B, Laschke MW, Rohan R, Koenig J, Menger MD (2001) *In vivo* imaging of physiological angiogenesis from immature to preovulatory ovarian follicles. Am J Pathol **159**: 1661-1670.

Wenger A, Stahl A, Weber H, Finkenzeller G, Augustin HG, Stark GB, Kneser U (2004) Modulation of *in vitro* angiogenesis in a three-dimensional spheroidal coculture model for bone tissue engineering. Tissue Eng **10**: 1536-1547.

Wenger A, Kowalewski N, Stahl A, Mehlhorn AT, Schmal H, Stark GB, Finkenzeller G (2005) Development and characterization of a spheroidal coculture model of endothelial cells and fibroblasts for improving angiogenesis in tissue engineering. Cells Tissues Organs **181**: 80-88.

Discussion with Reviewers

P. Habibovic: To further increase the impact of this work, it would be interesting to investigate the fate of implanted osteoblasts as well. These constructs are built to aid vascularisation of large bone tissue engineered constructs, and while indeed vascularisation is improved under HOB:HDMEC conditions, this is only useful if osteogenic differentiation or mineralisation of HOB cells is not negatively affected by the presence of endothelial cells.
Authors: We agree with the reviewer that it would be interesting to further analyse the influence of HDMEC on the differentiation and mineralisation potential of HOB. However, for this purpose, it may be more appropriate to use a large bone defect model for the implantation of the spheroids, which provides a more natural environment supporting osteogenic differentiation than the skinfold. In the case of the present study, we have intentionally chosen the dorsal skinfold chamber as the transplantation site for our spheroids, because this model allows for the repetitive *in vivo* visualisation of individual microvessels and, thus, vascularisation inside the grafts, which was the focus of our

experiments. Based on our promising results, we currently plan an additional study dealing with the performance of HOB containing spheroids as regenerative units in a large bone defect model.

P. Habibovic: Could you elaborate on the possible effect of agarose on the behaviour of cells inside spheroids? Would you expect a different response if another polymer is used?
Authors: In the present study, agarose was used during the generation of the spheroids by means of the liquid overlay technique. In this case, agarose solely served as a non-adherent surface to which the seeded cells could not attach and, thus, spontaneously aggregated to three-dimensional spheroids by developing cell-cell contacts. Accordingly, agarose was not incorporated into the spheroids, which only consisted of the used cell types. Therefore, it is not necessary to clarify in the present setting, if agarose or another polymer would have an effect on the behaviour of the cells inside the spheroids.

L. Kupczik: The authors write in the results section: "These microvessels were filled with erythrocytes over time by developing interconnections to the surrounding host microvasculature. However, they were not perfused with FITC dextran-labelled blood plasma at the time point of microscopic observation and, thus, appeared as black structures in the grafts. If the microvessels developed interconnections with the surrounding tissue, how is it possible that the FITC labelling did not penetrate into the intrinsic vessels but the erythrocytes did?
Authors: We assume that our microscopic observation is due to the fact that the erythrocytes and also non-stained blood plasma were able to enter the microvessels directly after the interconnection with the surrounding microvasculature. However, at this time point the newly developed microvascular networks of the spheroids did not necessarily exhibit many supplying and draining vessels guaranteeing sufficient blood perfusion. Accordingly, erythrocytes were trapped in the networks and further increased their resistance, inhibiting the inflow of FITC-dextran labelled blood plasma during the intravital microscopic analyses at the later time point.

L. Kupczik: Different media formulations were used in the *in vitro* phase. Could this affect the apoptotic behaviour of the cells (serum concentration, etc)? If so, this should be mentioned in the discussion.
Authors: We detected the highest number of apoptotic cells inside the HDMEC spheroids, which were generated and cultured under optimal media conditions for endothelial cells. In contrast, under suboptimal media conditions for endothelial cells used for the HOB-HDMEC group, we detected a significantly reduced number of apoptotic HDMEC. In addition, HOB-HDMEC-NHDF spheroids, which were also cultured under suboptimal media conditions, presented with a number of apoptotic cells which was comparable to optimally cultured HOB spheroids. Taken together, these findings indicate that the different media formulations did not negatively affect the apoptotic behaviour of the cells.

L. Kupczik: The thickness of these spheroid cultures is such that rate-limited mass transfer alone is sufficient to carry nutrients into the centre of the construct. Therefore, vascularisation is not essential for the viability of the cells. The findings presented here would be much more intriguing in a larger model. Is this construct scalable as it is? What modifications would be necessary to increase the size of the spheroid so that it would be useful for the purpose stated in the introduction (i.e., the repair of large bone defects)?
Authors: In the present study, the spheroids exhibited an initial diameter of ~500-700 µm 72 h after *in vitro* generation (see Fig. 3 of the article). After transplantation into the dorsal skinfold chamber, the spheroids changed their round shape, because they were positioned in between the host striated muscle tissue and the coverslip of the observation window of the chamber (see Fig. 8 of the article). Nonetheless, the thickness of the spheroids was larger than 200 µm. Because the amount of oxygen, which is required for cell survival, is limited to a diffusion distance of only ~150-200 µm from a supplying blood vessel (Folkman and Hochberg, 1973; Colton, 1995, text references), the initiation of vascularisation was still essential in our model to guarantee the long-term viability of the cells inside the spheroids.

In general, the size of the spheroids can easily be adjusted by varying the number of seeded cells per well when performing the liquid overlay technique. For instance, in a previous study we generated spheroids with a size of ~1200 µm by seeding 100,000 cells per well (Metzger *et al*., 2011, text reference). However, we do not feel that it is absolutely necessary to generate larger spheroids. In fact, it may be much easier to adequately fill irregularly shaped bone defects with many small spheroids. Moreover, smaller spheroids bear the advantage that they can be better incorporated into porous scaffolds, which are then implanted as tissue constructs into large bone defects (Laschke *et al*., 2013, text reference).